Vol 18 No 1, January 2009
1674-1056/2009/18(01)/0324-09

Chinese Physics B

© 2009 Chin. Phys. Soc.
and IOP Publishing Ltd

Growth mechanism and photoluminescence of the SnO_2 nanotwists on thin film and the SnO_2 short nanowires on nanorods*

Wang Bing(王 冰)† and Xu Ping(徐 平)

Shenzhen Key Lab of Micro-nano Photonic Information Technology, School of Electronic Science and Technology, Shenzhen University, Shenzhen 518060, *China*

(Received 16 June 2008; revised manuscript received 19 August 2008)

SnO_2 nanotwists on thin film and SnO_2 short nanowires on nanorods have been grown on single silicon substrates by using Au–Ag alloying catalyst assisted carbothermal evaporation of SnO_2 and active carbon powders. The morphology and the structure of the prepared nanostructures are determined on the basis of field-emission scanning electron microscopy (FESEM), transmission electron microscopy (TEM), selected area electronic diffraction (SAED), high-resolution transmission electron microscopy (HRTEM), x-ray diffraction (XRD), Raman and photoluminescence (PL) spectra analysis. The new peaks at 356, 450, and 489 nm in the measured PL spectra of two kinds of SnO_2 nanostructures are observed, implying that more luminescence centres exist in these SnO_2 nanostructures due to nanocrystals and defects. The growth mechanism of these nanostructures belongs to the vapour–liquid–solid (VLS) mechanism.

Keywords: nanostructures, crystal growth, photoluminescence
PACC: 7865K

1. Introduction

One-dimensional nanostructures such as wires, rods, and tubes have become the focus of intensive research due to their unique applications in mesoscopic physics and fabrication of nanoscale devices. For instance, they not only provide a good system to study the electrical and thermal transport in one-dimensional confinement, but also are expected to play an important role in both interconnection and functional units in fabricating electronic, optoelectronic, and magnetic storage devices with a nanoscale dimension.[1−4] It is well known that SnO_2 is an important functional material, which has been widely applied in the field of optoelectronics and microelectronics. For instance, SnO_2 can be utilized in solar cells,[5] transparent conducting electrodes,[6] gas sensors,[7,8], and transistors.[9] Naturally, to fabricate SnO_2-based nanoscaled devices, we are greatly challenged to prepare various nanoscaled building blocks with zero- to three-dimensions, e.g. particles, tubes or wires, and belts or junctions, for applications of nanomaterials. In recent years, the assembly and synthesis of zero- and one-dimensional SnO_2 nanostructures such as particles,[10] tubes,[11] and wires[12−23] has aroused the great interest. In this paper, we report two new kinds of SnO_2 nanostructures, i.e. nanotwists on thin film and short nanowires on nanorod, which grow on single silicon substrates by using Au–Ag alloying catalyst assisted carbothermal evaporation of SnO_2 powders.[24,25] Additionally, new peaks at 356, 450 and 489 nm in the measured photoluminescence spectra of SnO_2 nanostructures are observed, implying that more luminescence centres exist in these SnO_2 nanostructures due to nanocrystals and defects.

2. Experiment

The schematic diagram of the apparatus used in our experiment is shown in Fig.1. The synthesis of these SnO_2 nanostructures is depicted in detail as follows. The Au–Ag (atom ratio 1:1) layer (about 10 nm in thickness) is deposited on single silicon (001) substrates with an area of 5 mm^2 by using the sputtering technique. Note that we do not find silver to play any

*Project supported by the Fund of Shenzhen Key Lab of Micro-nano Photonic Information Technology, China (Grant No 2000811), the National Natural Science Foundation of China (Grant No 10704050) and Fok Ying Tung Educational Foundation (Grant No 114009).

†Corresponding author. E-mail: wangbing@szu.edu.cn

catalyst role in synthesizing the SnO_2 nanostructures in our case. The Au–Ag alloying target is employed in sputtering because the cost of the Au–Ag alloy is lower than that of the pure gold. The active carbon and SnO_2 powders (both 99.99% in purity) are mixed at a 1:4 weight ratio and loaded into a small quartz tube. The two Si substrates covered by Au–Ag alloy are positioned on a ceramic plate near the mixture of carbon and SnO_2 inside the small quartz tube. The spacing between two substrates is about 2 cm and substrate 1 is 2 cm away from the mixture of carbon and SnO_2. Then the small quartz tube with an inner diameter of 2.5 cm, is pulled into the centre of a large quartz tube with an inner diameter of 6 cm, and they are together inserted into a horizontal tube electric furnace. The whole system is evacuated by a vacuum pump for a couple of hours, and then the nitrogen gas is introduced into the system at a mass flow rate of 300 sccm, and the pressure is kept at about 5.3×10^4 Pa. Afterwards, the system is rapidly heated from room temperature up to 800°C and kept at the temperature for 10 min. Finally, the system is cooled down to room temperature in several hours. When two substrates are taken out of the small quartz, we can see grey production on substrates. Field-emission scanning electron microscopy (FESEM), transmission electron microscopy (TEM), selected area electronic diffraction (SAED), high-resolution transmission electron microscopy (HRTEM), x-ray diffraction (XRD) and the Raman spectrum are employed to identify the morphology and the structure of the synthesized products. Room-temperature photoluminescence (PL) is used to characterize the luminescence of these SnO_2 nanostructures. Note that we can easily repeat the experimental results, suggesting that our method is reliable and reproducible.

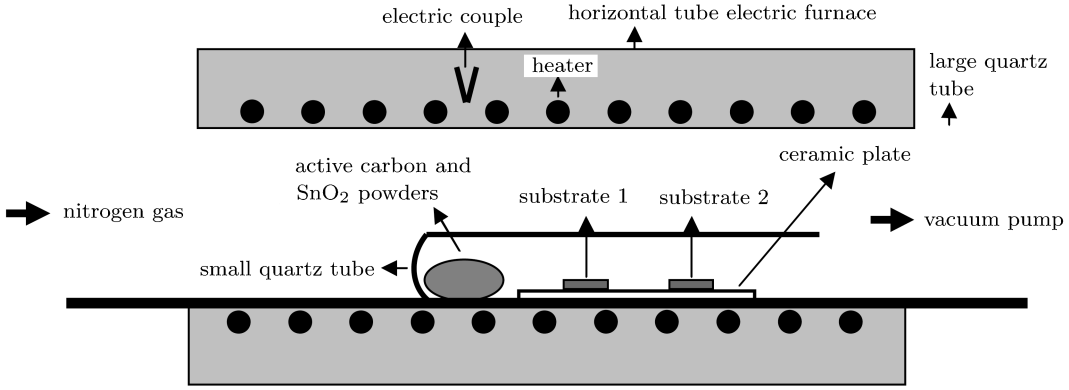


Fig.1. The schematic diagram of apparatus used in the experiment.

3. Result and discussion

Morphologies of the synthesized SnO_2 nanostructures in two substrates are shown in Figs.2 and 3. The morphologies of the structures in substrate 1 in Fig. 1 are displayed in Fig.2. From the FESEM image in Fig.2(a), we can see many SnO_2 nanotwists with diameters of 60–300 nm, lengths of 5–15 μm and the thin film has white dots with diameters of 200–800 nm. These SnO_2 nanotwists can be divided into two kinds of nanotwists, i.e. nanotwists with sections and nanotwists without sections. The lengths of sections in the nanotwists with sections are about 300 nm–1 μm. The details of the high-magnified FESEM images are displayed in Figs.2(b) and 2(c). In Fig.2(b), two SnO_2 nanotwists with sections are shown clearly. For the SnO_2 nanotwists with sections in the left, the diameter of each section is about 300 nm, and for that in the right, the diameter of each section is 200 nm. In both of SnO_2 nanotwists with sections, each section is of rutile-shape structure of SnO_2. In the border between the thin film and the nanotwist in the left, we can see clearly that there is a hole. One section of this nanotwist is inserted into this hole and connected with another section of the nanotwist. So we can draw a conclusion that the SnO_2 nanotwists with sections grows from the thin film. In Fig.2(c), one SnO_2 nanotwist without sections is clearly shown. The diameter of this nanotwist is about 250nm. In the border between this SnO_2 nanotwists and thin film, we can see clearly that there is a hole too. This nanotwist is inserted into this hole. So this SnO_2 nanotwist with sections

grows from the thin film too. The corresponding EDS spectrum recorded at the hole in Fig.2(b) is shown in Fig.2(d) and indicates that the root of the nanotwists with sections is mainly composed of Sn and Au (Ag and Si come from the Si substrate sputtered by Au–Ag alloy). The EDS pattern recorded at the hole in Fig.2(c) is basically the same as the result in Fig.2(d). The TEM bright-field image of the nanotwist without sections is shown in Fig.3(a). The size of this nanotwist without sections is about 80 nm. The corresponding HRTEM pattern recorded at one side of the nanotwist shows that the interplanar spacing is 0.262 nm corresponding to the (101) plane of a rutile SnO_2 lattice in Fig.3(b). Further, the corresponding SAED pattern in the left-bottom of Fig.3(b) recorded with an electron beam perpendicular to the long axis of the nanotwist demonstrates that this nanotwist is a single crystal with a rutile structure and grows along the [$\bar{2}$00] direction.

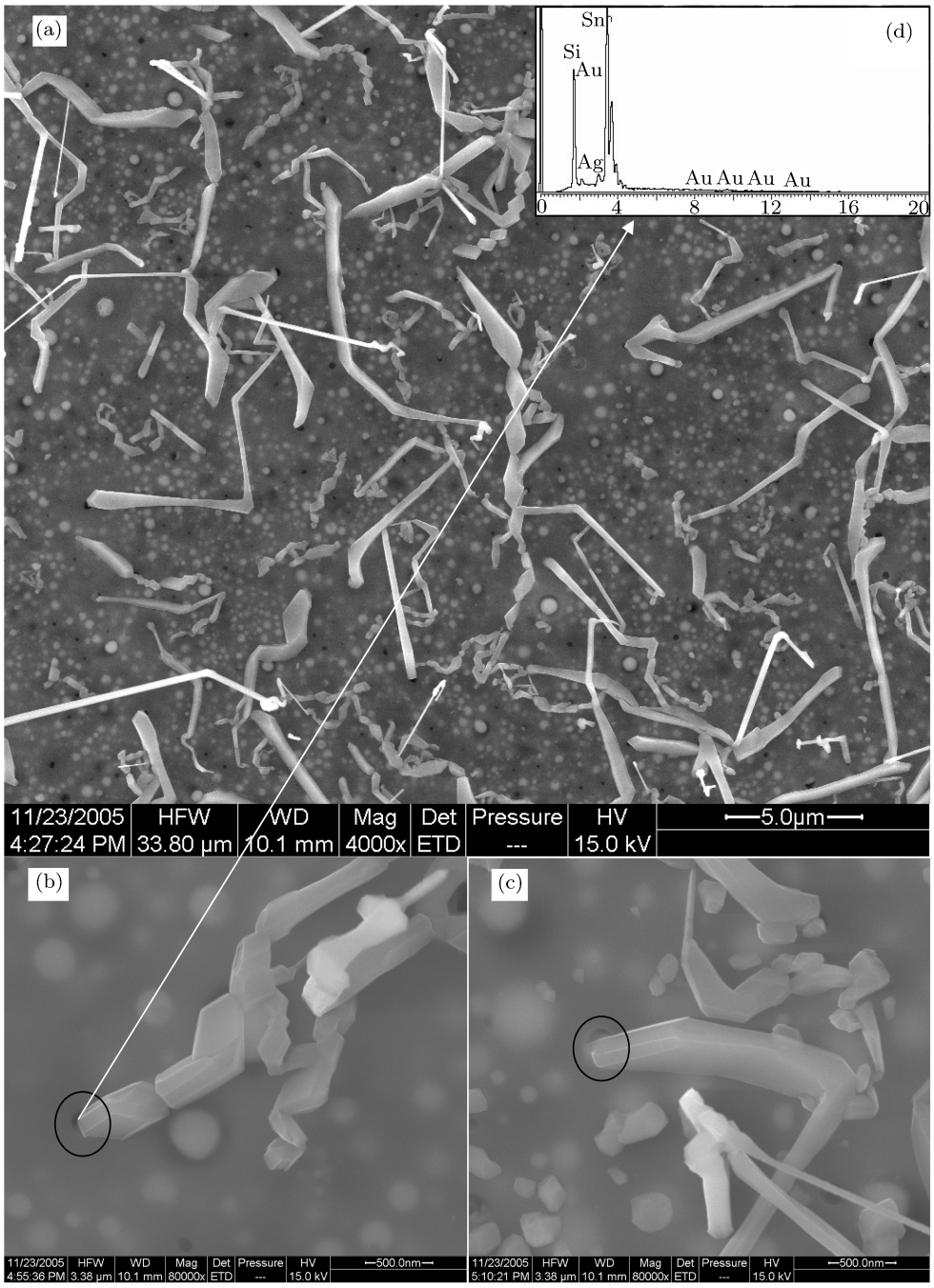


Fig.2. FESEM image of the synthesized SnO_2 nanotwists on thin film (a), (b), (c) and the EDS pattern of the root of the nanotwists with sections on thin film (d).

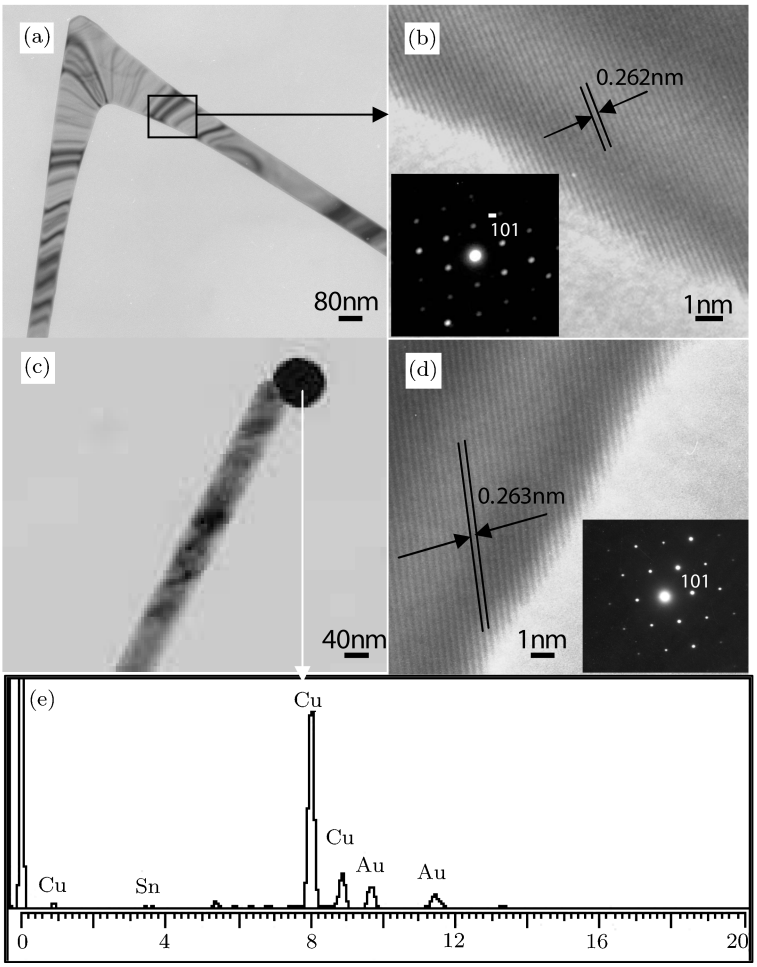


Fig.3. TEM Bright-field image of the synthesized SnO_2 nanotwists without sections on thin film (a), the corresponding HRTEM image and the SAED pattern of the nanotwist recorded with the electron beam along the $[0\bar{1}0]$ direction (b), TEM Bright-field image of the synthesized SnO_2 short nanowire with a nanopowder at the root of the nanowire (c), the corresponding HRTEM image and the SAED pattern of the short nanowires recorded with the electron beam along the $[0\bar{1}0]$ direction (d), and the EDS pattern of the nanopowder at the root of the nanowire (e).

The morphologies of the structures in substrate 2 in Fig.1 are displayed in Fig.4. From the FESEM image in Fig.4(a), we can see the short SnO_2 nanowires and nanorods arranged in a branch shape. The magnified FESEM images are shown in Figs.4(b) and 4(c), where the short nanowires growing from the nanorods are clearly displayed. The diameters of the short nanowires are about 30–100 nm and their lengths are about 1–4 μm. On the tip of each nanowire, there is a small ball with a diameter between 100–120 nm. The higher-magnified FESEM image in Fig.4(d) shows that the diameters of nanorods are about 100–130 nm. These nanorods are distributed beside the core axis, thereby forming the branch-shape structure. The TEM bright-field image of a short nanowire with a nanopowder at the root of the nanowire is shown in Fig.3(c). The size of this short nanowire is about 50nm. The corresponding HRTEM pattern recorded at one side of the short nanowire shows that the interplanar spacing is 0.263 nm corresponding to the (101) plane of a rutile SnO_2 lattice in Fig.3(d). Further, the corresponding SAED pattern in the right-bottom of Fig.3(d) recorded with an electron beam perpendicular to the long axis of the short nanowire demonstrates that this short nanowire is a single crystal with a rutile structure and grows along the [200] direction. The corresponding EDS spectrum shown in Fig.3(e) recorded at the nanopowder in the root of the short nanowire indicates that the nanopowder is mainly composed of Sn and Au (Cu comes from the TEM grid).

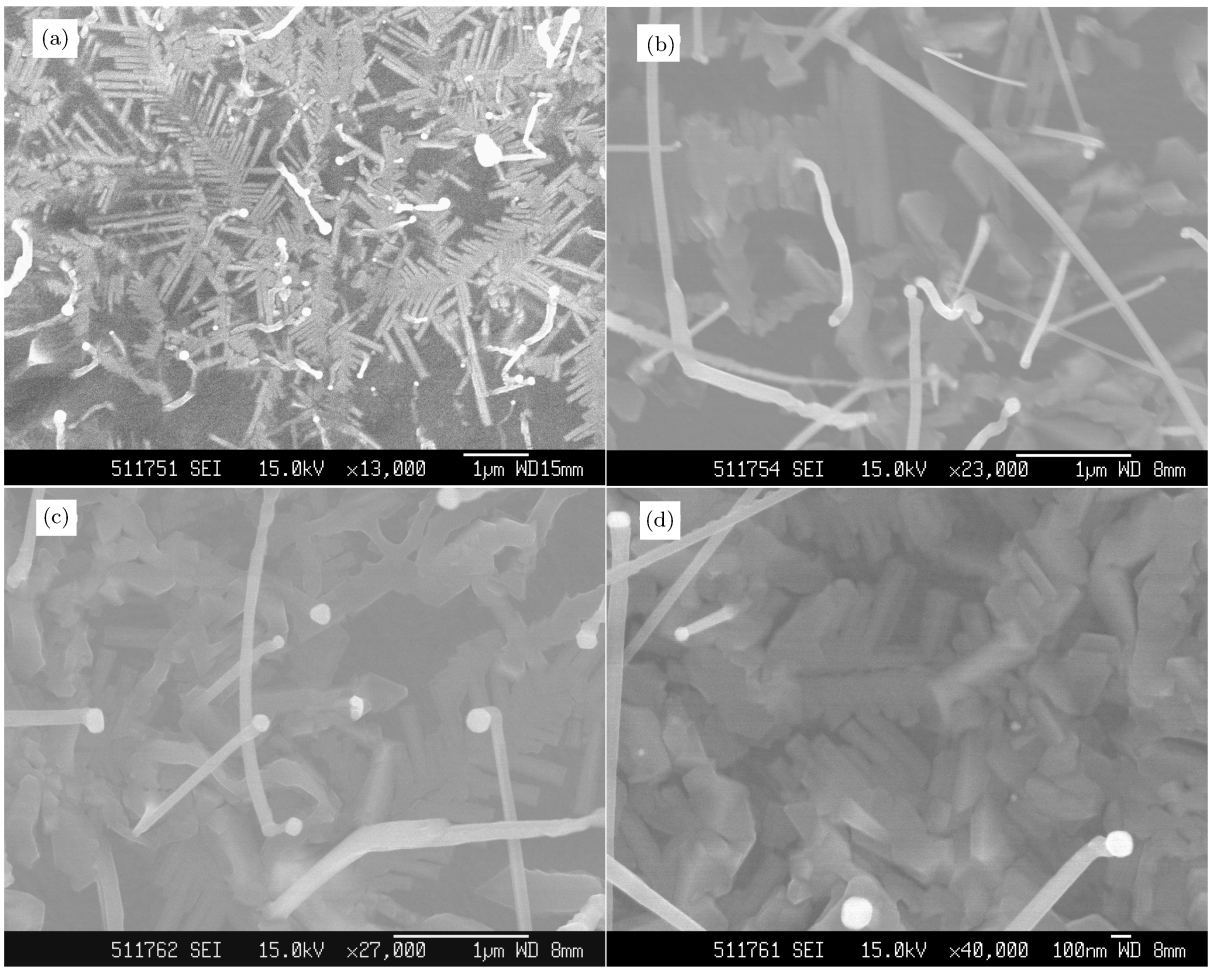


Fig.4. FESEM images (a), (b), (c) and (d) of the synthesized SnO_2 short nanowires on nanorods.

The x-ray diffraction (XRD) measurement is carried out to identify the crystalline structures of the two kinds of SnO_2 nanostructures, and Fig.5 shows the XRD patterns. Both SnO_2 samples show a tetragonal rutile SnO_2 phase with (110), (101), (200), (111), (210), (211), (220), (002), (310), (301), (202) and (321) diffraction peaks. The XRD patterns of the samples indicate that the crystalline structural parameters can be indexed to the tetragonal rutile structure of SnO_2 with lattice constants of a=0.4738 nm and c=0.3188 nm (JCPDS 21-1250). In addition, the diffraction peak at 2θ=69.02° is quite broad due to the overlapping with that of Si (400) in the XRD pattern of the SnO_2 short nanowires on nanorods. In the XRD pattern of the SnO_2 nanotwists on thin film, metallic body-centred tetragonal β-Sn phase (lattice parameters a=0.583 nm, and b=0.318 nm) with (200), (101), (220) and (211) diffraction peaks appears, which comes from the white dots in the thin film.

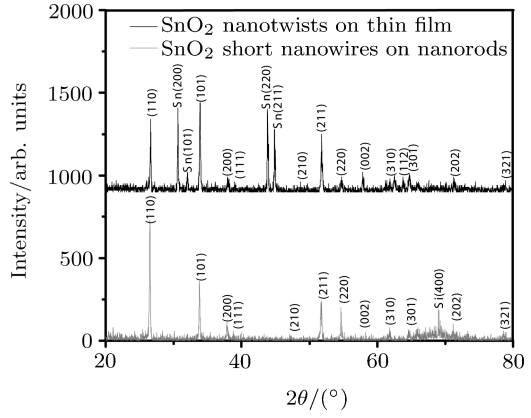


Fig.5. The XRD patterns of the synthesized SnO_2 nanostructures.

The room temperature Raman scattering spectra of SnO_2 nanostructures in two samples are shown in Fig.6. Rutile SnO_2 belongs to the space group D_{4h}^{14}, of which the normal lattice vibration at the Γ point of the Brillouin zone is given on the basis of group theory:[26] $\Gamma = 1A_{1g} + 1A_{2g} + 1A_{2u} + 1B_{1g} + 1B_{2g} + 2B_{1u} + 1E_g + 3E_u$. Among them, the four first-order active Raman modes are B_{1g}, E_g, A_{1g} and B_{2g}, and the active IR modes are A_{2u}, E_u and B_{1u}. In the room temperature Raman scattering spectra (Fig.5) of the SnO_2 thin films, three fundamental Raman peaks at 470, 630 and 771 cm^{-1} are displayed, which respectively correspond to E_g, A_{1g} and B_{2g} vibration modes.[27] Thus, these peaks further confirm that the as-synthesized SnO_2 thin films possess the feature of the tetragonal rutile structure. In addition, the two weak Raman bands of 496 and 689 cm^{-1} seem to correspond, respectively, to IR-active A_{2u} TO and A_{2u} LO (LO denotes the mode of the longitudinal optical photos, and TO refers to the mode of the transverse optical photos) modes, which are similar to $E_{u(2)}$TO of SnO_2 nanopowders and $E_{u(2)}$LO of SnO_2 nanorods respectively.[28–30] Furthermore, the peak at 540 cm^{-1} is identified to be of S_2 mode, which is believed to be the consequence of the disorder activation of SnO_2 nanotwists on thin film.[31] Finally, the peak at 520 cm^{-1} is the characteristic peak of the Si substrate for the sample of SnO_2 short nanowires on nanorods while this peak does not appear in the XRD pattern of SnO_2 nanotwists on thin film, which is attributed to the bareness of the Si from the interval of the nanorods arranged and the thin thickness of the nanorod level in substrate 2 as compared with the thickness of the thin film in substrate 1.

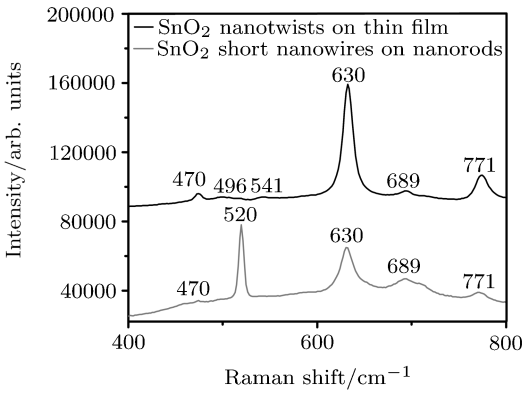


Fig.6. The Raman spectra of the synthesized SnO_2 nanostructures.

PL spectra of the obtained SnO_2 nanostructures in two samples are investigated at room temperature, and the result is shown in Fig.7. Both the PL spectra of the SnO_2 nanotwists on thin film and the PL spectra of the SnO_2 short nanowires on nanorods consist of the emission band located at 356, 401, 416, 450, 470, 489, 551 and 575 nm. Firstly, the peak at 343 nm is the band-to-band emission peak of the two kinds of SnO_2 nanostructures, which originates from the recombination of free exciton of electron–hole.[32] That the peak does not appear is due to the fact that the peaks caused by defects associated with oxygen vacancies or tin interstitials resulting from the size effect of the SnO_2 nanostructures are strong, thereby crippling the band-to-band emission peak.[33] Secondly, the appearance of the 401 nm peak is independent of the concentration of oxygen vacancies, but it is due to structural defects or luminescent centres, such as nanocrystals or defects in the SnO_2 nanostructures.[33,34] Thirdly, the peak at 470 nm is possibly attributed to the electron transition mediated by defect levels such as oxygen vacancies in the band gap.[35] Fourthly, the 416, 551, and 575nm peaks have been observed in previous reports.[24,36–38] In addition, the PL spectra of the SnO_2 nanotwists on thin film consist of the emission band located at 370 nm. The 370 nm peak is attributed to the band-to-acceptor peak and related to the impurity or defect concentration, but not to the structural properties.[34] Finally, the 356, 450, and 489 nm peaks are newly found in our case, and they should be from new luminescence centres existing in two SnO_2 nanostructures, such as nanometre-sized crystals and defects.[27]

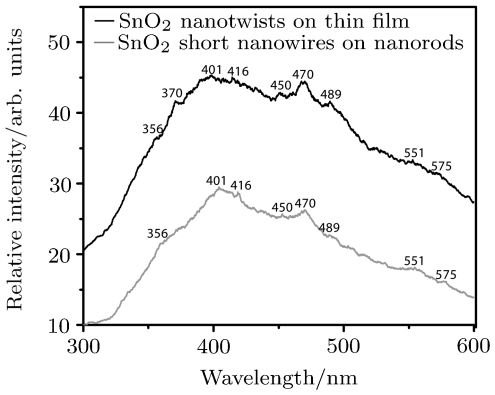


Fig.7. The room temperature PL spectra of the synthesized SnO_2 nanostructures.

The growth mechanism of SnO_2 nanostructures can be explained on the basis of the vapour–liquid–solid (VLS) processes, and the growth process is shown in Fig.8. In experiment, Au in Au–Ag alloy

as a catalyst is usually used to promote the formation of SnO_2 nanostructures. For the SnO_2 nanotwists on thin film, the growth process is described in Figs.8(a)–8(d) in sequence. In the first stage formed is the SnO_2 thin film covering the Sn–Au alloy and the Si substrate, which can be proved by the EDS pattern shown in Fig.2(d). SnO_2 powders first react with the active carbon in a high temperature region in furnace, thereby producing SnO. Subsequently, the produced SnO decomposes into Sn and SnO_2 in a low temperature region in the furnace. Sn droplets are still in a liquid state at the reaction temperature due to their low melting point (231.9°C) and fall on the substrate and form Sn–Au alloyed droplets by reacting with the Au particles.[31] Meanwhile, SnO_2 from the reaction (1) can envelop into Sn–Au alloying droplets and the surface of the Si substrate can turn into a thin film covering the Sn–Au alloy and the surface of Si substrate as shown in Fig.8(a). In the second stage formed is the thin film hole on the Sn–Au alloy as shown in Fig.8(b). Due to the temperature-dependent volume expansion of Sn inside Sn–Au alloying droplets and the confinement from the outer solid thin film of SnO_2, the high internal pressure of the Sn–Au alloy leads the thin film of SnO_2 on the alloy to protuberate outward.[39] When the inner pressure goes up to the endurance limit of the SnO_2 thin film, the internal Sn will break through the SnO_2 thin film and spout out, thereby forming a hole in the thin film as shown in Fig.8(b). In the third stage, the SnO_2 nanostructure is formed on the thin film. These Sn–Au alloying droplets can provide the energetically favourable sites for the adsorption of SnO_2 vapour,[37] so the SnO_2 dissolves in the alloying droplets. The continuous dissolution of SnO_2 results in a supersaturated solution.[40] Ultimately, the SnO_2 nanostructure grows out by precipitation of SnO_2 from the supersaturated droplets as shown in Fig.8(c). Note that this kind of growth belongs to the bottom growth of the VLS growth mechanism, because the catalyst of Sn–Au alloy droplet is in the bottom of the nanostructure and connect with the Si substrate. Formed in the final stage is the SnO_2 nanotwist without sections or SnO_2 nanotwist with sections as shown in Fig.8(d). If the nanostructure in Fig.8(c) grows out from the thin film and converts into the SnO_2 nanotwist without sections, the growth direction may change from the initial direction to other direction, in whose corresponding growth crystal plane the surface free energy lower than that of the initial growth crystal plane can change the growth direction of nanostructure from the initial direction to other direction, thereby forming a nanotwist without sections. For the SnO_2 nanotwist with sections, the growth mechanism is not clear and will being studied in future.

For the SnO_2 short nanowires on nanorods, the growth process is described in Figs.8(e)–8(h) in sequence. In the first stage the SnO_2 nanorods are formed as shown in Fig.8(e). The growing mechanism of these nanorods is suggested to be of VLS process. SnO_2 powders first react with the active carbon, producing SnO. Subsequently, the produced SnO decomposes into Sn and SnO_2. Sn droplets are still in a liquid state at the reaction temperature due to their low melting point (231.9°C) and fall on the substrate and form alloyed droplets by reacting with the Au particles.[31] Simultaneously, these alloying droplets can provide the energetically favourable sites for the adsorption of SnO_2 vapour, so the SnO_2 dissolves in the alloying droplets. The continuous dissolution of SnO_2 results in a supersaturated solution.[40] Ultimately, the SnO_2 nanorods grow out by precipitation of SnO_2 from the supersaturated droplets. In the second stage the Sn droplets on the nanorods are formed as shown in Fig.8(f). Sn has a low melting point, so it can easily condense on any surface such as the surfaces of the synthesized SnO_2 nanorods and form Sn droplets in our case. In the third stage the SnO_2 short nanowire is formed on the nanorods as shown in Fig.8(g), which can be proved by the EDS pattern shown in Fig.3(e). The Sn droplets can provide the energetically favourable sites for the adsorption of SnO_2 vapour,[41] so the SnO_2 dissolves in the alloying droplets. The continuous dissolution of SnO_2 results in a supersaturated solution.[40] Ultimately, the SnO_2 short nanowires grow out by precipitation of SnO_2 from the supersaturated droplets on the synthesized nanorods. Note that this kind of growth belongs to the top growth of the VLS growth mechanism, because the Sn droplets, as catalyst, are on the tops of the short nanowires and do not connect with the nanorods. Finally, with the growth of the short nanowires, the SnO_2 short nanowires form on nanorods as shown in Fig.8(h).

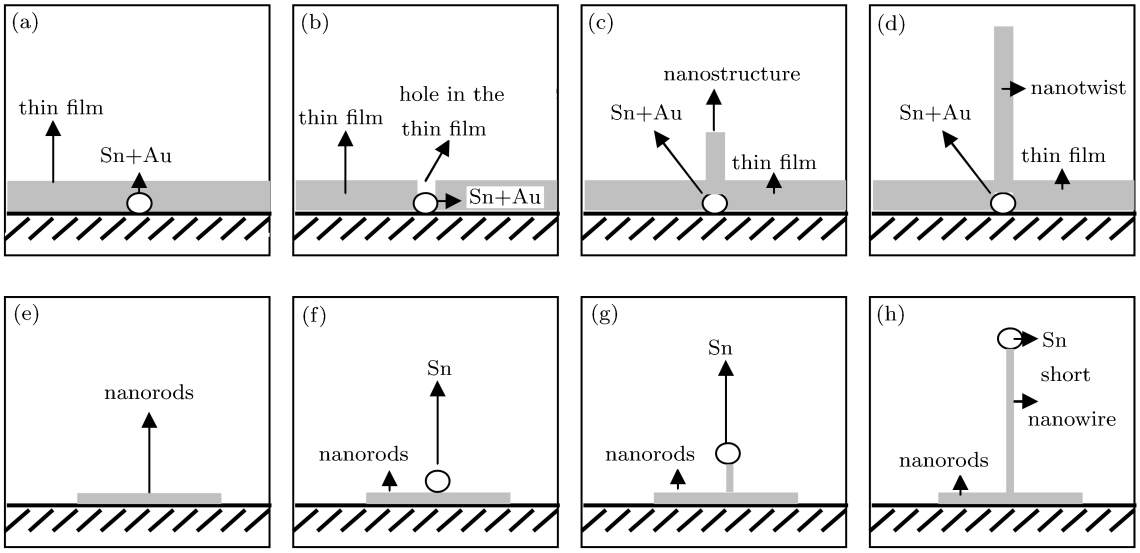


Fig.8. The growth mechanism of the synthesized SnO_2 nanostructures.

Additionally, the different distances of the samples from the reaction source of active carbon and SnO_2 powders could lead to the different substrate temperatures, which is one of the main factors causing different synthesized morphologies of SnO_2 nanostructures in the two substrates. Naturally, the degree of supersaturation of the alloying droplets plays an important role in forming nanostructure due to the difference in substrate temperature.[24]

4. Conclusion

SnO_2 nanotwists on thin film and SnO_2 short nanowires on nanorods have been synthesized on single silicon substrates by using Au–Ag alloy assisted carbothermal evaporation of SnO_2 and active carbon powders. The new peaks at 356, 450, and 489 nm in the measured photoluminescence spectra of SnO_2 nanostructures are observed, implying that more luminescence centres exist in these SnO_2 nanostructures due to nanocrystals and defects. The growth mechanism of these nanostructures belongs to the VLS mechanism.

Acknowledgement

The authors thank the State Key Laboratory of Optoelectronic Materials and Technologies, School of Physics Science & Engineering, Zhongshan University, Guangzhou, China for providing the experimental facilities.

References

[1] Xia Y, Yang P, Sun Y, Wu Y, Mayers B, Gates B, Yin Y, Kim F and Yan H 2003 *Adv. Mater.* **15** 353

[2] Hu M and Qin Y X 2008 *Acta Phys. Sin.* **57** 3698

[3] Cao J W, Deng Z Q, Huang Y H, Liao Q L and Zhang Y 2008 *Acta Phys. Sin.* **57** 3641

[4] Fang L M, Liu C M, Zhou W L and Zu X T 2007 *Chin. Phys.* **16** 95

[5] Ferrere S, Zaban A and Gregg B A 1997 *J. Phys. Chem.* B **101** 4490

[6] He Y S, Cambell J C, Murphy R C, Arendt M F and Swinnea J S 1993 *J. Mater. Res.* **8** 3131

[7] Ansari G, Boroojerdian P, Sainkar S R, Karekar R N, Alyer R C and Kulkarni S K 1997 *Thin Solid Films* **295** 271

[8] Varghese O K and Malhotra L K 1998 *Sens. Actuat.* B **53** 19

[9] Duan X F, Huang Y, Cui Y, Wang J and Leiber C M 2001 *Nature* **409** 66

[10] Leite E R, Weber I T, Longo E and Varela J A 2000 *Adv. Mater.* **12** 965

[11] Iijima S 1991 *Nature* **375** 769

[12] Liu Y K, Zheng C L, Wang W Z, Yin C R and Wang G H 2001 *Adv. Mater.* **13** 1883

[13] Feldman Y, Wasserman E, Srolovitz D J and Tenne R R 1995 *Science* **267** 222

[14] Dai H J, Wong W E, Yu Y Z, Fan S S and Lieber C M 1995 *Nature* **375** 769
[15] Pan Z W, Lai H L, Duan X F, Zhou W Y, Shi W S, Wang N N, Lee C S, Wong N B, Lee S T and Xie S S 2000 *Adv. Mater.* **12** 1186
[16] Wang Z L, Dai Z R, Gao R P, Bai Z G and Gole J L 2000 *Appl. Phys. Lett.* **77** 3349
[17] Han W, Fan S, Li Q and Hu Y 1997 *Science* **277** 1287
[18] Duan X F and Leiber C M 2000 *J. Am. Chem. Soc.* **122** 188
[19] Han W Q, Fan S S, Li Q Q, Gu B L, Zhang X B and Yu D P 1997 *Appl. Phys. Lett.* **71** 2271
[20] Duan X F and Leiber C M 2000 *Adv. Mater.* **12** 298
[21] Duan X.F, Huang Y, Cui Y, Wang J and Leiber C M *Nature* **409** 66
[22] Morales A M and Leiber C M 1998 *Science* **279** 208
[23] Lee S T, Wang N, Zhang Y F and Yang Y H 1999 *Mater. Res. Soc. Bull.* **24** 36
[24] Wang B, Yang Y H, Wang C X and Yang G W 2005 *Chem. Phys. Lett.* **407** 347
[25] Wang B, Yang Y H, Wang C X and Yang G W 2005 *J. Appl. Phys.* **98** 073520
[26] Porto S P S, Fleury P A and Damen T C 1967 *Phys. Rev.* **154** 522
[27] Sun S H, Meng G W, Zhang G X, Gao T, Geng B Y, Zhang L D and Zuo J 2003 *Chem. Phys. Lett.* **376** 103
[28] Peng X S, Zhang L D, Meng G W, Tian Y T, Lin Y, Geng B Y and Sun S H 2003 *Vacuum* **93** 1760
[29] Liu Y K, Zheng C L, Wang W Z, Yin C R and Wang G H 2001 *Adv. Mater.* **13** 1883
[30] Abello L, Bochu B, Gaskov A, Koudryavtseva S, Lucazeau G and Roumyantesva M 1998 *J. Solid State Chem.* **135** 78
[31] Wang J X, Liu D F, Yan X Q, Yuan H J, Ci L J, Zhou Z P, Gao Y, Song L, Liu L F, Zhou WY, Wang G and Xie S S 2004 *Solid State Commun.* **130** 89
[32] Lee E J H, Ribeiro C, Giraldi T R, Longo E and Leite E R 2004 *Appl. Phys. Lett.* **84** 1745
[33] Kimand T W and Lee D U 2000 *J. Appl. Phys.* **88** 3759
[34] Jeong J, Choi S P, Chang C, Shin D C, Park J S, Lee B T, Park Y J and Song H J 2003 *Solid State Commun.* **127** 595
[35] Gu F, Wang S F, Lu M K, Zhou G. J, Xu D and Yuan D R 2004 *J. Phys. Chem.* B **108** 8119
[36] Wang B, Yang Y H, Wang C X, Xu N S and Yang G W 2005 *J. Appl. Phys.* **98** 124303
[37] Wang B, Yang Y H and Yang G W 2006 *Nanotechnology* **17** 5916
[38] Wang B, Yang Y H and Yang G W 2006 *Nanotechnology* **17** 4682
[39] Moseler M and Landman U 2000 *Science* **289** 1165
[40] Chen Y Q, Cui X F, Zheng K, Pan D Y, Zhang S Y, Wang B and Hou J G 2003 *Chem. Phys. Lett.* **369** 16
[41] Hansen M and Anderko K 1958 *Constitution of Binary Alloys* (New York: McGraw-Hill) p36